Improvement of Insulation Effectiveness of Natural Rubber by Adding Hydroxyl-Functionalized Barium Titanate Nanoparticles

Neudys González
Departament d'Enginyeria Química, Universitat Politècnica de Catalunya, Av. Diagonal 647, 08028 Barcelona, Spain

Jordi-Roger Riba
Departament d'Enginyeria Elèctrica, Universitat Politècnica de Catalunya, Rambla Sant Nebridi 22, 08222 Terrassa, Spain

Maria dels Àngels Custal
Sicame Company, C/ Zinc, 14 – Polígono Industrial Aquiberia, 08755, Castellbisbal, Barcelona, Spain

and **Elaine Armelin**
Departament d'Enginyeria Química, Universitat Politècnica de Catalunya, Av. Diagonal 647, 08028 Barcelona, Spain
Center for Research in Nano-Engineering, Universitat Politècnica de Catalunya, Campus Sud, Edifici C', C/Pasqual i Vila s/n 08028 Barcelona, Spain

ABSTRACT

Natural rubber (NR) products are being applied in many protective tools for life-line applications, including insulating boots, blankets, sleeves, insulating gloves, or flexible coverings. Due to the inherent risk of such works it is imperative ensuring the quality of the safety products involved. The dielectric properties of NR-based products rely heavily on the compounding formulation and manufacturing processes involved. Considerable efforts are being applied to improve the dielectric performance of NR formulations to ensure that maintenance personnel work in the safer and most comfortable conditions. This work studies the addition of different weight fractions of surface-modified $BaTiO_3$-OH nanoparticles to NR formulations to enhance dielectric properties such as breakdown strength and leakage current. The results presented in this work show that the addition of a low weight fraction of surface-modified $BaTiO_3$-OH nanofillers (≤ 1 wt.%) enhances the surface and volume resistivity, crystallinity, breakdown strength under ac conditions and lowers the leakage current under dc stress.

Index Terms — **Breakdown, leakage current, dielectric test, nanoparticles, natural rubber, live-line maintenance.**

1 INTRODUCTION

HIGH voltage applications require insulating materials exhibiting improved dielectric properties [1], such as enhanced breakdown voltage, low leakage current and high reliability. Life-line maintenance works are conducted in live conditions, that is, in energized power systems, so safety issues are a top priority for personnel involved. Live-line maintenance is essential to minimize outage occurrence in critical points of the power system and ensure power system reliability and availability. Live-line maintenance must ensure workers' safety, thus eliminating the possibility of being energized [2]. This objective is achieved by applying specific safety techniques and using appropriate rubber barriers that prevent workers' exposure against current paths. Such protective tools include insulating boots, blankets, sleeves, insulating gloves, or flexible coverings, among others, which often are made of highly insulating natural rubber (NR) compounds [3]. The amount of leakage current flowing through the insulation greatly determines the level of safety [4].

When properly compounded and cured, NR is an effective thermostable insulating material with appealing mechanical features such as high elasticity and flexibility, mechanical fatigue and tearing resistance and good hydrophobicity. However, the final dielectric properties of NR depend strongly on the processes involved in NR technology and the compounding formulation, which includes a rather large number of inorganic and organic materials such as fillers, anti

Manuscript received on 22 July 2016, in final form 16 January 2017, accepted 25 May 2017. Corresponding author: J.-R. Riba.

degradants, plasticizers, vulcanizing agents or accelerators among others. It is well-known that the insulation effectiveness offered by most insulating products increases with their thickness. Considerable efforts are being done to increase the dielectric performance of NR formulations while minimizing the thickness of the resulting protective tools such as insulating gloves and sleeves. By this way the comfort, effort and touch can be greatly improved during object manipulation by wearers [5]. Recently, we have reported that by using specific nanofillers in the NR recipe, the dielectric properties of the final products can be strongly improved [6].

Nanocomposites exhibit improved mechanical, thermal, and electrical insulating properties than conventionally filled polymers. These appealing features allow designing more reliable and compact insulating tools, with a significant cost reduction. Therefore, to obtain improved dielectric materials based on polymer nanocomposites, nanoparticles technology must maturate to obtain improved dielectric features [7]. The electric field strength at breakdown in nonpolar polymeric materials such as NR composites depends upon field-dependent charge carrier density and mobility, as well as to the trapping probability. The dielectric breakdown is also influenced by thermal and electromechanical conditions which can induce dielectric breakdown at lower electric field strength [8]. Ferroelectric ceramics such as $BaTiO_3$ exhibit reduced dielectric loss [9] than other materials and higher permittivity due to dipolar effects. These effects confer extra polarization to the ferroelectric ceramics under the application of an electric field, although at values beyond the coercive field a significant permittivity reduction is observed due to material saturation [8]. According to the mixtures law the increase of the effective permittivity of the composite is small at low $BaTiO_3$ volume fractions. However, higher volume fractions tend to reduce both the mechanical properties and the breakdown electric field strength [9]. The dielectric properties of the composite material are related to the shape and size of the fillers, their volume fractions or the processing methods among others [10]. Polymer composites with substantial structural inhomogeneity tend to exhibit reduced dielectric performance [11]. The distortion of the local electric field due to the presence of particles within the polymeric matrix is greatly influenced by the size of such particles. The smaller the particles are, the poorer the electric field enhancement, assuming the same filler volume fraction. Therefore, the addition of nanoparticles results in better dielectric performance than the addition of microparticles [12]. The improvement of the dielectric behavior is in part owing to the greater nanofiller surface area, and in part because of the slower dynamics of the polymer chains surrounding the minuscule aggregates [13].

The agglomeration of fillers agglomeration tends to form conductive pathways which in turn increase the dielectric loss and the leakage current [14]. Therefore, in order to boost the dielectric properties it is vital to obtain a homogeneous microstructure [15], avoiding agglomerates that could increase the material porosity, thus boosting electron conduction and dielectric loss [11]. In [1] it is reported that nanofiller agglomerates tend to enhance the electrical conductivity and polarization current of the material due to the increase of the concentration of the moving charges. Valera-Zaragoza et al [16] reported that to obtain good interaction between TiO_2 particles and the NR matrix, the particles must have nanometric size even though the interfacial adhesion they experiment tend to generate large agglomerates that reduce the dielectric performance of such composites [17]. The dielectric properties are improved when nanofillers are added to the NR formulation compared to pure NR [7]. However, when dealing gradually incrementing the nanofiller content, at a certain threshold limit there is a sudden increment of the electrical conductivity and dielectric loss [18], known as the percolation threshold. This phenomenon is attributed to the development of conductive pathways through the aggregated nanofillers within the insulating polymeric matrix when the filler content exceeds the percolation threshold. It is also known that beyond the percolation threshold, the leakage current within the nanocomposites raises [19] and the dielectric breakdown strength lowers [17]. In this limit situation, the fillers tend to contact with each other, thus forming a continuous cluster that extends throughout the polymeric matrix. It can result in important changes of the physical properties which no longer follow the linear law of mixtures [20].

Although several works report on the use of barium titanate ($BaTiO_3$) nanoparticles as filler in insulating polymeric materials such as silicone rubber [21], very few works report on the application of such nanosize fillers in NR products. Surface functionalization of the nanoparticles is a convenient approach to improve dispersion of the nanoparticles within the nanocomposite structure since it allows reinforcing the interfacial interaction between the polymeric matrix and the nanoparticles [17]. Surface modification of the nanoparticle fillers produces a surface coating layer that increases the electric field strength at breakdown and lowers the dielectric loss [22]. Yu et al [23] reported that the addition of surface modified $BaTiO_3$ particles in poly(vinylidene fluoride) enhances the dielectric properties and reduces dielectric loss, even at high filler loading. Choudhury [11] stated that the addition of active hydroxyl –OH groups on the surface of the $BaTiO_3$ particles produces a more uniform dispersion of the nanoparticles in a polyetherimide matrix, thus increasing the low-frequency dielectric permittivity and decreasing dielectric loss. The addition of $BaTiO_3$–OH nanofillers can also significantly reduce the leakage current density through the poly(vinylidenefluoride trifluoroethylene) composite while enhancing the dielectric breakdown strength and the effective permittivity [17].

There are few works studying the use of low concentration of $BaTiO_3$ surface-functionalized nanoparticles in NR to be used to manufacture safety tools for live-line maintenance applications. This work aims at analyzing the dielectric properties of the NR formulations when adding different weight fractions of hydroxylated $BaTiO_3$ nanoparticles under both ac and dc stress conditions.

2 MATERIALS

High purity $BaTiO_3$ nanopowder (purity ≥ 99%) with an

average size less than 100 nm and hydrogen peroxide solution (30% w/w) were acquired from Sigma Aldrich Chemicals (Spain), whereas NR resins were purchased from several suppliers and used as received. Other reagents and additives in the latex formulation were of commercial grade.

The surface hydroxylation of $BaTiO_3$ nanoparticles was performed by refluxing the nanoparticles in an aqueous solution of H_2O_2 at 105 ºC (24h), following a procedure similar to that reported in [24]. Suitable conversion from the unmodified nanoparticle to the hydroxylated form of $BaTiO_3$ was followed by the appearance of the absorption bands at ~3400 cm^{-1} and 1000-1100 cm^{-1}, which were assigned, respectively, to the –OH stretching and bending vibrations in the infrared spectra [25] (see Fig. 1). Therefore, the presence of O-H hydrogen bond absorption bands corroborates that nanoparticles surfaces were successfully functionalized.

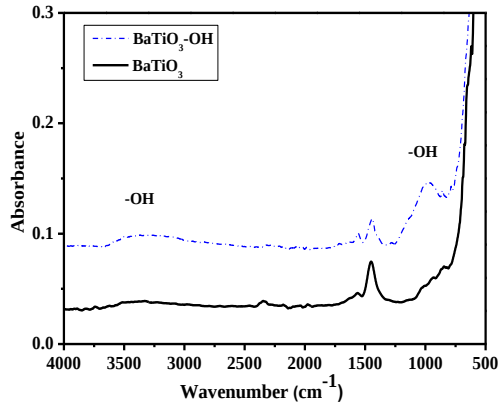

Figure 1. FTIR spectra of unmodified $BaTiO_3$ nanoparticles and $BaTiO_3$ nanoparticles functionalized with H_2O_2.

NR-based $BaTiO_3$-OH nanocomposites were prepared according to the method described by Li et al [24]. A solution containing the latex emulsion was placed in a 250 mL three-neck flask and slightly stirred by means of a mechanical stirrer. The other additives (accelerators, vulcanizing agent, fillers and antioxidant) were dispersed in an aqueous solution prior to addition to the NR emulsion and afterwards were carefully sonicated. A quantitative amount of hydroxyl-functionalized $BaTiO_3$ was mixed with a dispersant agent (Cab-o-Sperse® solution) with vigorous stirring and further sonicated for 10 min to obtain a homogeneous and viscous solution. Finally, it was added to the latex emulsion and mixed with a mechanical stirrer.

Fig. 2 represents the surface hydroxylation of $BaTiO_3$ nanoparticles and the particle–matrix interaction.

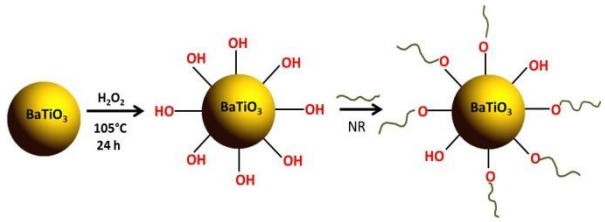

Figure 2. Surface functionalization of $BaTiO_3$ nanoparticles and addition to the latex emulsion to obtain the nanofilled polymer composite.

The test tubes used as mold were dipped in the latex suspension and then dried in an oven at 75 ºC for 3 h (pre-vulcanizing step). The complete curing was obtained after gradually washing the samples in a bath with distilled water from 25 to 70 ºC, and then baked for 24 h at 75ºC. Finally, the specimens were cooled to room temperature and peeled off from the glass tubes, thus obtaining the NR-functionalized $BaTiO_3$ solid nanocomposite films (0.95–1.05 mm of thickness). A set of NR/$BaTiO_3$ nanocomposite films with $BaTiO_3$-OH contents of 0.25, 0.5, 1.0, 5.0 and 10 wt.%, respectively, were prepared by repeating the above explained procedure.

Fourier transform infrared spectra were recorded using a FTIR 4100 Jasco spectrophotometer in the absorbance mode within the spectral range of 600−4000 cm^{-1}. The FTIR analysis was employed to characterize the nanoparticles.

To investigate the incorporation of functionalized $BaTiO_3$ in the NR matrix, X-ray diffraction (XRD) 2θ scans were performed by means of a Bruker D8 Advance diffractometer, using CuKα radiation (λ = 0.15406 nm), equipped with one-dimensional LynxEye detector.

The Autolab PGSTAT 302N apparatus was used to measure the dielectric response of the analyzed samples. It is an impedance analyzer specially designed to conduct EIS (Electrochemical Impedance Spectroscopy) measurements with 1 MHz bandwidth, ± 10 V voltage range, ± 2 A current range and current and voltage accuracies ± 0.2%. All experiments were carried at room temperature using a capacitor cell as in [26] and circular NR samples (1.5 cm of diameter, 700 µm of thickness).

The surface and volume resistivity of the NR samples were measured with an HP 4329A high-resistance meter coupled to an Agilent HP 16008A resistivity cell. A constant dc voltage of 500V for 1 min (followed by 5 min of discharge mode) or 5 min (followed by 30 min of discharge mode) was applied. Measurements were done at room temperature (20 ± 1ºC) with a relativity humidity below 70%. Resistivity measurements were performed to NR disks of 12 cm of diameter and 1 cm of thickness.

A Phenix BK130/36 variable high-voltage transformer was used to carry out the ac dielectric tests. It allows selecting two output voltage ratings, that is, 0-36 kV and 0-130 kV. The Phenix BK130/36 includes precision voltage and current metering to fulfill the requirements of both the ASTM D120 [27] and IEC-60903 [28] standards. Two Phenix 4120-10 dc hipots incorporating voltage and current metering were used for the dc dielectric tests. They provide positive and negative variable voltage output respectively, within the range 0-120 kV.

An optical microscope Olympus BXS1 was used to check the failed zones of the composite specimens as well as to measure the average diameter of the perforations. The morphology of the NR samples with and without hydroxylated $BaTiO_3$ nanoparticles were investigated after dielectric experiments using a Focus Ion Beam Zeiss Neon 40 (Carl

Zeiss) scanning electron microscope (SEM). Morphologies were visualized at an accelerating voltage of 5 kV, whereas energy-dispersive X-ray (EDX) analyses were performed at 3 kV.

3 RESULTS

This section describes the different tests carried out to characterize the NR specimens used as reference and the NR nanocomposite samples with 0.25, 0.50, 1.0, 5.0 and 10.0 % weight fractions of hydroxylated $BaTiO_3$ nanofillers.

3.1 X-RAY DIFFRACTION (XRD)

The crystalline structure of the samples analyzed can be characterized by means of X-ray diffraction (XRD) [9]. The degree of crystallinity in polymers characterizes the portion of ordered molecules inside the polymer matrix. It is known that the dielectric permittivity increases significantly with the proportion of free radicals into the polymeric matrix [29] and decreases when increasing the degree of crystallinity. Therefore nonpolar polymeric matrixes tend to exhibit lower dielectric constant and dielectric loss [30].

Fig. 3 shows the results attained with the XRD technique. Since NR is a nonpolar polymer, only a broad peak is expected in the XRD analysis, corresponding to the amorphous phase from polymer chains (2θ = 10°-30°). The intense peaks in the $BaTiO_3$-OH diffraction pattern shown in Fig. 3 are indicative of the highly ordered crystalline structure of such material, homogenously distributed within the vulcanized NR films.

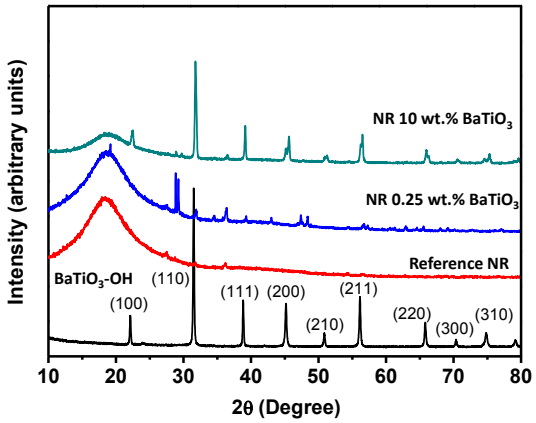

Figure 3. X-ray diffraction patterns of functionalized $BaTiO_3$-OH nanoparticles and natural rubber composites with the minimum and maximum weight fractions of $BaTiO_3$-OH filler.

3.2 SURFACE AND VOLUME RESISTIVITY

Direct current volume and surface resistivity of the samples analyzed were characterized according to the ASTM D257 standard [31]. Results presented in Tables 1 and 2 show that both surface and volume resistivity of the NR formulations increase when increasing the content of $BaTiO_3$-OH nanofillers up to 0.5 wt.%, but beyond this threshold value the electrical properties tend to decrease.

Table 1. Surface resistivity.

	$\sigma_{1\ minute,\ 500\ V}$ ($x10^{15}\ \Omega$)	$\sigma_{5\ minute,\ 500\ V}$ ($x10^{15}\ \Omega$)
Reference NR sample	0.19 ± 0.03	7.56 ± 0.22
0.25 wt.% $BaTiO_3$-OH	0.49 ± 0.03	2.11 ± 0.22
0.50 wt.% $BaTiO_3$-OH	1.95 ± 0.09	10.50 ± 0.28
1.0 wt.% $BaTiO_3$-OH	1.70 ± 0.02	4.46 ± 0.98
5.0 wt.% $BaTiO_3$-OH	1.34 ± 0.04	4.09 ± 0.37
10.0 wt.% $BaTiO_3$-OH	0.96 ± 0.02	3.63 ± 0.09

Table 2. Volume resistivity.

	$\rho_{1\ min,\ 500\ V}$ ($x10^{15}\ \Omega$·cm)	$\rho_{5\ min,\ 500\ V}$ ($x10^{16}\ \Omega$·cm)
Reference NR sample	1.19 ± 0.04	1.10 ± 0.50
0.25 wt.% $BaTiO_3$-OH	1.39 ± 0.03	2.82 ± 0.08
0.50 wt.% $BaTiO_3$-OH	5.94 ± 0.84	15.50 ± 0.49
1.0 wt.% $BaTiO_3$-OH	3.65 ± 0.17	8.40 ± 0.50
5.0 wt.% $BaTiO_3$-OH	2.34 ± 0.26	6.91 ± 0.26
10.0 wt.% $BaTiO_3$-OH	1.60 ± 0.04	4.15 ± 0.30

3.3 ELECTROCHEMICAL IMPEDANCE SPECTROSCOPY (EIS)

To conduct EIS experiments, the samples were immersed in a distilled water solution with NaCl 3.5 wt.% at 20 ± 1 ºC for 24 hours. The water excess was removed by using a special tissue before introducing the samples in the measuring cell [26]. The complex permittivity of the analyzed samples soaked with the NaCl solution was then calculated, whose real and imaginary parts are shown in Figures 4 and 5, respectively. Figure 6 shows the loss tangent of the analyzed samples.

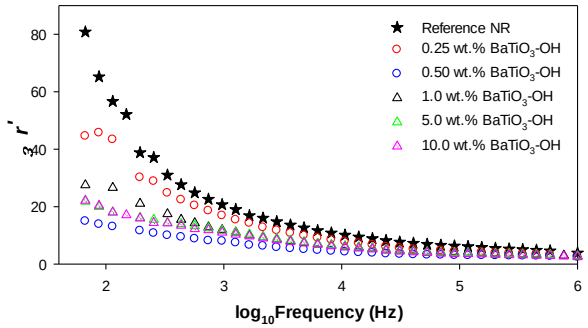

Figure 4. Real part of the complex permittivity in the 50 Hz – 1MHz frequency range of the analyzed samples soaked with 3.5 wt.% NaCl solution.

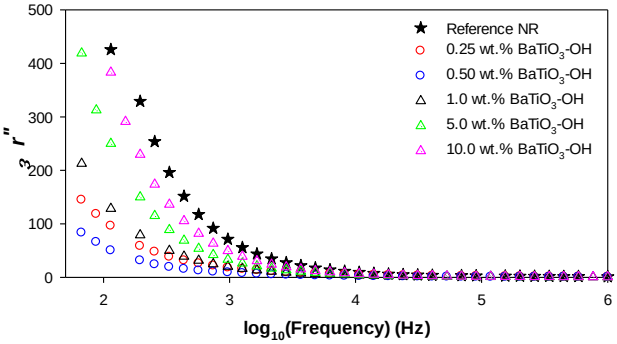

Figure 5. Imaginary part of the complex permittivity in the 50 Hz – 1MHz frequency range of the analyzed samples soaked with 3.5 wt.% NaCl solution.

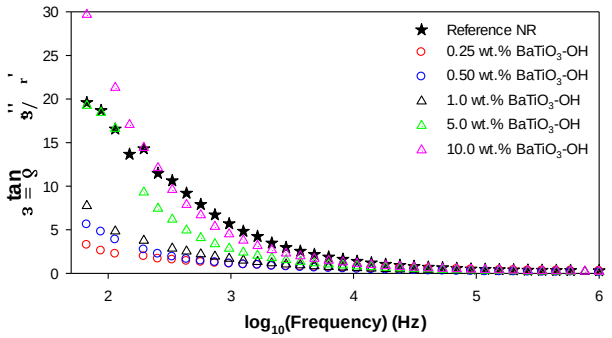

Figure 6. Loss tangent in the 50 Hz - 1 MHz frequency range of the analyzed samples soaked with 3.5 wt.%. NaCl solution.

Results presented in Fig. 4 show that the addition of low volume fractions of surface modified BaTiO3 nanofillers lowers the dielectric constant in the low frequency interval. Results presented in Fig. 5 suggest that all studied $BaTiO_3$ surface-functionalized nanocomposite formulations, and especially those with lower filler concentration, have smaller imaginary part of the permittivity in the low frequency interval and hence they should exhibit lower dielectric loss and leakage current than the reference NR samples [32]. Fig. 6 proves that the samples incorporating a low volume fraction of $BaTiO_3$-OH nanofillers exhibit lower tanδ.

3.4 DIELECTRIC TESTS

Figure 7 shows the experimental setup used to perform the dielectric tests. The voltage was raised continuously from 0 V up to breakdown conditions, and both the applied voltage and leakage current were measured in several points to obtain the graphs shown in Figures 8, 9 and 10. To deal with the inherent variability among samples, three samples of each formulation with an approximate thickness of 1 mm were tested. To account for small thickness deviations, both the leakage current and voltage were normalized to 1 mm thickness.

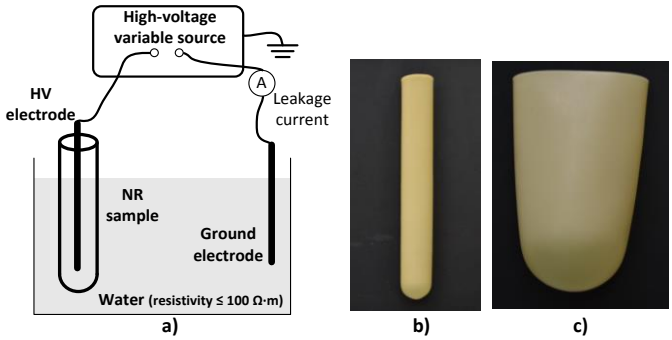

Figure 7. a) Schematics of the dielectric withstand tests. b) Specimens used in the ac dielectric tests; height = 80 mm, diameter = 16.5 mm. c) Specimens used in the dc dielectric tests; height = 80 mm, diameter = 51.05

It is known that under ac stress, insulating materials such as NR often present two differentiated conduction mechanisms [33]. When applying a low electric field, the charge carriers can be either electrons or ions and the ohmic conduction mechanism prevails. Under these conditions the insulating material follows the Ohm's law and there is a linear relationship between the applied electric field and the current density. However, under intense electric field conditions, that is, when its strength is sufficient to overcome the potential barriers between the contacts and the polymer there is a non-linear relationship between the electric field in the sample and the current density [33]. The relationship between the current density and the electric field strength is often written as a two-term equation, the first term owing to the low-field ohmic conduction mechanism and the second one due to the high-field non-linear SCLC (space charge limited current) conduction term [33],

$$J = \sigma E + A \cdot E^2 \quad (1)$$

E being the electric field strength upon the insulating sample, σ the electric conductivity of such material and A a parameter derived from the Mott-Gumey law for planar solid dielectrics that defines the single carrier SCLC [33]–[35],

$$A = \frac{9}{8} \cdot \frac{\varepsilon_0 \varepsilon_r \mu}{d} \quad (2)$$

μ being the mobility of the charge carriers, ε_0 and ε_r the permittivity of free space and the relative dielectric permittivity of the polymer, respectively, and d the thickness of the polymeric sample.

The dielectric breakdown of the NR material used in safety tools for live-line maintenance occurs due to the SCLC development. Therefore, by using appropriate NR formulations the mobility of the charge carriers can be reduced and thus the breakdown electric field strength can be increased [33].

Figure 8 and Table 3 summarize the results of the ac dielectric tests for both the reference NR samples and the samples including different weight fractions of $BaTiO_3$-OH nanofillers.

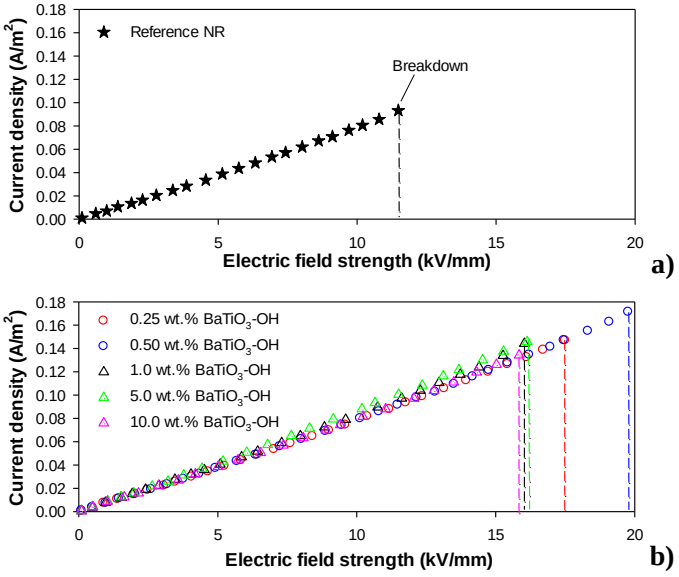

Figure 8. Alternating current dielectric tests. Current density versus electric field strength response curves (RMS values). a) Reference NR sample. b) Diverse NR-based composites with different weight fractions of $BaTiO_3$-OH nanofillers.

Table 3. Parameters arising from equation (1).

	σ [μA/(m·V)]	A [(A/V^2)x10^{-12}]	R^2

Reference NR sample	7.074e-3	8.408e-5	0.99984
0.25 wt.% $BaTiO_3$-OH	7.101e-3	7.121e-5	0.99994
0.50 wt.% $BaTiO_3$-OH	7.153e-3	7.253e-5	0.99993
1.0 wt.% $BaTiO_3$-OH	7.453e-3	8.581e-5	0.99971
5.0 wt.% $BaTiO_3$-OH	8.044e-3	6.197e-5	0.99996
10.0 wt.% $BaTiO_3$-OH	7.193e-3	7.791e-5	0.99983

Results from Figure 8 and Table 3 clearly show that although the slope of the *J-E* curves is quite similar for all analyzed samples, which provides useful information about the electrical conductivity of the material, the breakdown electric field strength is dramatically raised for all NR-based composites with different volume fractions of $BaTiO_3$-OH nanofillers. The breakdown electric field strength is an important property in insulating materials intended for high-voltage systems. As explained, the addition of inorganic fillers can substantially change its magnitude, depending on filler type, concentration, size and dispersion, surface modification or dielectric characteristics of such fillers. Therefore the filler fraction in nanodielectric composites needs to be controlled to increase the dielectric strength [36]. The results presented here suggest that the addition of low weight fractions of about 0.5 wt.% of surface modified $BaTiO_3$-OH nanofillers is beneficial since it allows reducing the SCLC mechanisms occurring under high electric fields, which eventually leads to dielectric breakdown of the material.

Analogously to ac dielectric withstand tests, direct current (dc) tests of both polarities were carried out by means of two Phenix 4120-10 dc hipots, one with positive output and the other with negative output. It is known that charge injection at the electrodes and electroluminescence phenomena generate charge carriers which tend to accumulate within the polymeric material, forming a space charge [37]. Space charge in dielectrics is mostly generated under dc stress [38], although its effects cannot be totally ignored under ac conditions. Space charge generates dissipative loss, reduces the withstand voltage, intensifies the local electric field and can produce insulation failure [37]. The addition of small volume fractions of nanofillers can reduce the space charge extent [8], [39], [40] this effect being especially notorious at low filler concentration [41], thus enhancing the volume resistivity. The tendency to suppress charge injection is believed to be due to deep trap mechanisms [42] that capture the charge injected by the electrodes, thus, reducing the electrical conduction [43] by inhibiting charge injection and avoiding space charge buildup. Deep traps are formed because of the interfacial interactions between the organic polymeric matrix and the inorganic nanoparticles, which at the nanoscale range are very strong since nanoparticles exhibit a very high surface area to volume ratio. Therefore, the atoms placed on the surface of the material tend to be more reactive than the atoms placed in the bulk. In conclusion, the interface plays a fundamental role to determine the electrical behavior of nanodielectrics [41]. When the energy of the captured charges is not enough to flee from the deep traps, the leakage current is lowered.

Results attained in the dc dielectric tests are summarized in Figures 9 and 10, for positive and negative polarity, respectively. Results presented in Figures 9 and 10 clearly show a great reduction of the leakage current of the $BaTiO_3$ surface-functionalized nanocomposite samples when compared to the reference NR samples. This could be due to the effect of the deep traps introduced by the modified $BaTiO_3$-OH nanofillers, which also lead to a reduction of the imaginary part of the permittivity (dielectric loss), as shown in Figure 5. Polymers with high dielectric loss also have high leakage current since they convert electrical into thermal energy [44]. However, the electric field at breakdown is not improved or even slightly decreased due to the addition of nanofillers with different dielectric constant than that of the polymer matrix [8, 44, 45].

Figures 9 and 10 show a slightly different behavior of the analyzed samples under positive and negative dc polarity tests. This difference can be due to the inherent polarization and surface polarization mechanisms, the mobility and recombination mechanisms of electronic and ionic charge carriers or the effect of impurities and structural defects [46]. The results presented in Figs. 9 and 10 are in close agreement with those reported in [47]–[49].

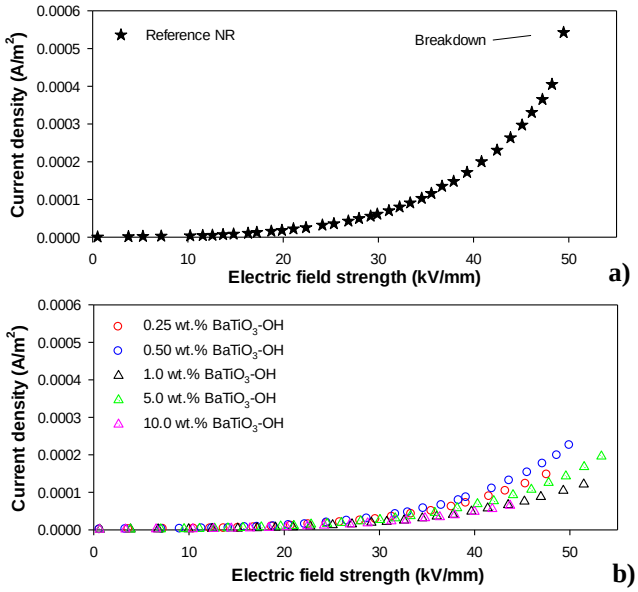

Figure 9. Positive dc polarity dielectric tests. Current density versus electric field strength response curves. a) Reference NR sample. b) Diverse NR-based composites with different weight fractions of $BaTiO_3$-OH nanofillers.

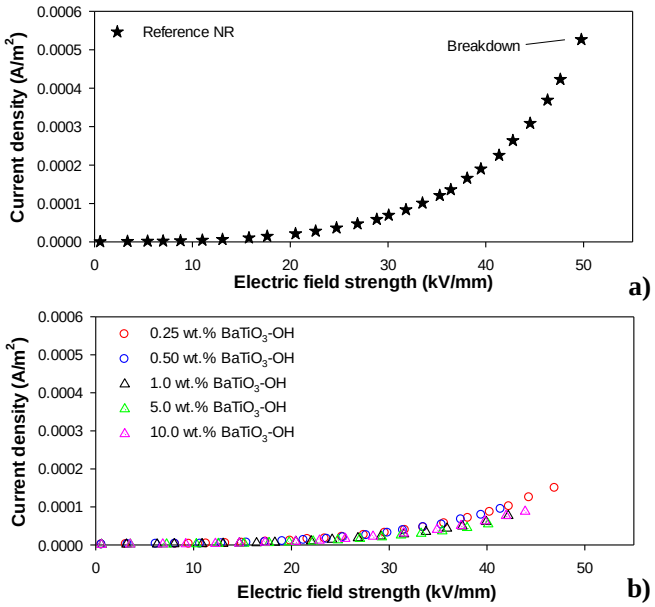

Figure 10. Negative dc polarity dielectric tests. Current density versus electric field strength response curves. a) Reference NR sample. b) Diverse NR-based composites with different weight fractions of $BaTiO_3$-OH nanofillers.

Figures 11 and 12 show, respectively, optical and SEM micrographs of different perforations formed as a consequence of the breakdown tests. These images clearly prove that the perforations are produced in areas with an anomalous concentration of agglomerates. Figures 11 and 12 corroborate that the dispersion of the compounding elements is of paramount importance to obtain high-quality products, especially at high filler loading. By comparing Figure 12a (reference NR sample with microfillers) with Figure 12b (sample with $BaTiO_3$ nanoparticles) it is deduced that a better dispersion of the particles produces perforations with smoother and more uniform edges. Then, the presence of nanoparticles also improves the electric field distribution within the polymeric matrix [50], thus enhancing the dielectric properties and the electric field strength at breakdown. Thus, it is of critical importance to achieve an excellent dispersion of all fillers during the production stages.

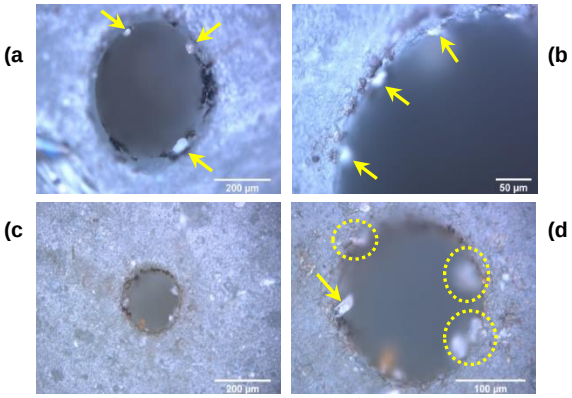

Figure 11. Optical photographs of the perforation produced by the dielectric breakdown on the reference NR sample. Alternating current polarization. a) Magnification x20. b) Magnification x50. Direct current polarization. c) Magnification x20. d) Magnification x50. Arrows and dashed circles indicate the presence of filler particles.

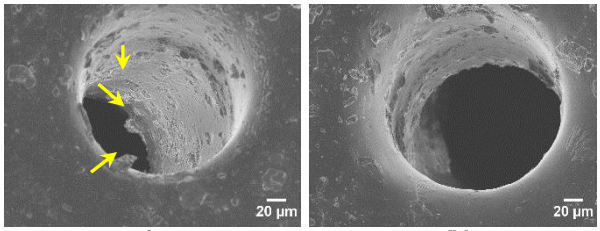

Figure 12. Scanning electron microscopy (SEM) images of the perforation produced by the dielectric breakdown in DC: a) NR unmodified sample. b) NR sample with 10 wt.% BaTiO3-OH nanofillers. Arrows indicate the presence of agglomerates of fillers checked by EDX (energy-dispersive X-ray spectroscopy).

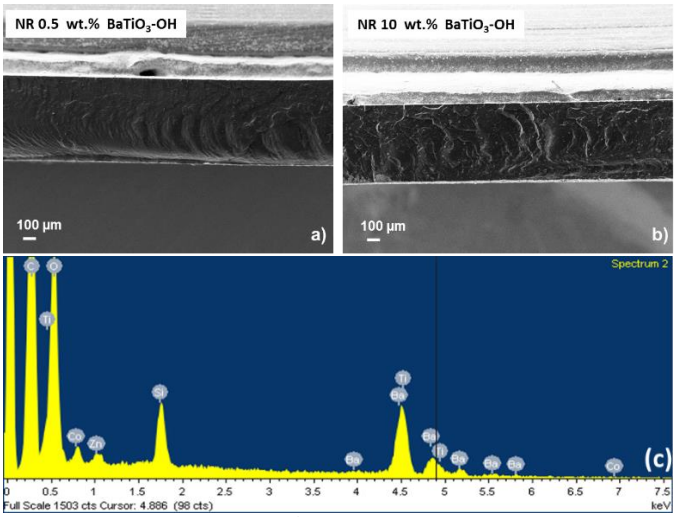

Figure 13. SEM micrographs of NR/$BaTiO_3$-OH nanocomposites: (a) NR sample with 0.5 wt.% $BaTiO_3$-OH , (b) NR sample with 10 wt.% $BaTiO_3$-OH and c) EDX spectrum of 10 wt.% NR/$BaTiO_3$-OH composite.

The inspection of the cryo-fractured surfaces of NR samples was performed by means of scanning electron microscopy (SEM) analysis (see Figs. 13a and 13b) followed by image analysis. The calculated polydispersity was about 4% for 0.5 wt.% $BaTiO_3$-OH samples, and about 42% for 10 wt.% $BaTiO_3$-OH samples. These results clearly indicate lower homogeneity and dispersion of the 10 wt.% $BaTiO_3$-OH samples. Additionally, $BaTiO_3$ nanofillers can be easily detected by EDX analysis, as shown in Fig. 13c.

4 CONCLUSION

This work has analyzed the improvement of the dielectric properties of NR formulations after the incorporation of different concentrations of hydroxylated $BaTiO_3$ nanoparticles. XRD results have proved that samples containing hydroxyl-functionalized $BaTiO_3$ nanoparticles present a more ordered crystalline structure. Measurements performed under dc stress have shown improved surface and volume resistivity of NR samples even with small volume fractions of $BaTiO_3$-OH nanofillers. Dielectric tests under ac stress conditions suggest that the addition of 0.5 wt.% of modified $BaTiO_3$-OH nanoparticles allows increasing the breakdown strength, which is attributed to a drop of the SCLC mechanisms arising under high electric fields. Dielectric tests carried out under dc

voltage of both polarities have proved a great reduction of the leakage current of the $BaTiO_3$ surface-functionalized nanocomposite samples with low weight fractions compared to the reference NR samples. This behavior has been attributed to the effect of the deep traps introduced by the modified $BaTiO_3$-OH nanofillers. Finally, SEM micrographs have proved that nanosize fillers and ultrasonication dispersion are the keys for improving insulation effectiveness of NR composites. Conversely, agglomerates act as defects, thus actuating as centers of electric field enhancement and insulation aging. Results derived from this work can be useful to improve the dielectric properties of NR-based safety tools used in different high-voltage products intended for life-line maintenance works.

ACKNOWLEDGMENT

This work has been supported by the Generalitat de Catalunya (Spain) within the Industrial Doctorate program. Neudys González acknowledges the fellowship (2013DI036) promoted by the Industrial Doctorate program.

REFERENCES

[1] N. A. M. Jamail, M. A. M. Piah, N. A. Muhamad, Z. Salam, N. F. Kasri, R. A. Zainir; and Q. E. Kamarudin, "Effect of Nanofillers on the Polarization and Depolarization Current Characteristics of New LLDPE-NR Compound for High Voltage Application," Adv. Mater. Sci. Eng., Vol. 2014, pp. 1–7, 2014.

[2] G. Cain, "Rubber-insulating goods," IEEE PES 12th Int'l. Conf. Transmission and Distribution Construction, Operation and Live-Line Maintenance (ESMO), pp. 1–8, 2011.

[3] S. Shunmugam, "Live maintenance in high voltage substations: Malaysia's experience," 11th Int'l. Conf. Live Maintenance (ICOLIM), pp. 1–4, 2014.

[4] M. Amin, S. Amin, and M. Ali, "Monitoring of leakage current for composite insulators and electrical devices," Rev.Adv.Mater.Sci, Vol. 21, pp. 75–89, 2009.

[5] R. Wells, S. Hunt, K. Hurley, and P. Rosati, "Laboratory assessment of the effect of heavy rubber glove thickness and sizing on effort, performance and comfort," Int'l. J. Ind. Ergon., Vol. 40, No. 4, pp. 386–391, 2010.

[6] N. González, M. del À. Custal, S. Lalaouna, J.-R. Riba, and E. Armelin, "Improvement of dielectric properties of natural rubber by adding perovskite nanoparticles," Eur. Polym. J., Vol. 75, pp. 210–222, 2016.

[7] R. V. Prakash;, B. G. Babu;, and D. E. Selvaraj, "Analysis of Relative Permittivity and Tan Delta Characteristics of Silicone Rubber Based Nano-composites," Int. J. Sci. Eng. Technol., Vol. 1, No. 5, pp. 201–206, 2012.

[8] P. Tewari, "Interfacial effects in oxide-polymer laminar composite thin film dielectrics for capacitor applications," Ph.D. Thesis, The Pennsylvania State University, USA, 2009.

[9] Z. Zepu Wang, J. K. Nelson, J. Jianjun Miao, R. J. Linhardt, L. S. Schadler, H. Hillborg, and S. Su Zhao, "Effect of high aspect ratio filler on dielectric properties of polymer composites: a study on barium titanate fibers and graphene platelets," IEEE Trans. Dielectr. Electr. Insul., Vol. 19, No. 3, pp. 960–967, 2012.

[10] A. Ladhar, M. Arous, H. Kaddami, M. Raihane, A. Kallel, M. P. F. Graça, and L. C. Costa, "AC and DC electrical conductivity in natural rubber/nanofibrillated cellulose nanocomposites," J. Mol. Liq., Vol. 209, pp. 272–279, 2015.

[11] A. Choudhury, "Preparation, characterization and dielectric properties of polyetherimide nanocomposites containing surface-functionalized BaTiO3 nanoparticles," Polym. Int'l., Vol. 61, No. 5, pp. 696–702, 2012.

[12] D. Ma, R. W. Siegel, J.-I. Hong, L. S. Schadler, E. Mårtensson, and C. Önneby, "Influence of Nanoparticle Surfaces on the Electrical Breakdown Strength of Nanoparticle-Filled Low-Density Polyethylene," J. Mater. Res., Vol. 19, No. 3, pp. 857–863, 2004.

[13] S. Javadi, M. Sadroddini, M. Razzaghi-Kashani, P. N. B. Reis, and A. A. Balado, "Interfacial effects on dielectric properties of ethylene propylene rubber–titania nano- and micro-composites," J. Polym. Res., Vol. 22, No. 8, p. 162, 2015.

[14] S. Yu, F. Qin, G. Wang, "Improving the dielectric properties of poly(vinylidene fluoride) composites by using poly(vinyl pyrrolidone)-encapsulated polyaniline nanorods," J. Mater. Chem. C, Vol. 4, No. 7, pp. 1504–1510, 2016.

[15] S. A. Paniagua, Y. Kim, K. Henry, R. Kumar, J. W. Perry, and S. R. Marder, "Surface-Initiated Polymerization from Barium Titanate Nanoparticles for Hybrid Dielectric Capacitors," ACS Appl. Mater. Interfaces, Vol. 6, No. 5, pp. 3477–3482, 2014.

[16] M. Valera-Zaragoza, A. Yescas-Yescas, E. A. Juarez-Arellano, A. Aguirre-Cruz, A. Aparicio-Saguilán, E. Ramírez-Vargas, S. Sepúlveda-Guzmán, and S. Sánchez-Valdes, "Immobilization of TiO2 nanoparticles on montmorillonite clay and its effect on the morphology of natural rubber nanocomposites," Polym. Bull., Vol. 71, No. 6, pp. 1295–1313, 2014.

[17] M. N. Almadhoun, U. S. Bhansali, and H. N. Alshareef, "Nanocomposites of ferroelectric polymers with surface-hydroxylated BaTiO3 nanoparticles for energy storage applications," J. Mater. Chem., Vol. 22, No. 22, p. 11196, 2012.

[18] S. Luo, S. Yu, R. Sun, and C.-P. Wong, "Nano Ag-Deposited BaTiO 3 Hybrid Particles as Fillers for Polymeric Dielectric Composites: Toward High Dielectric Constant and Suppressed Loss," ACS Appl. Mater. Interfaces, Vol. 6, No. 1, pp. 176–182, 2014.

[19] N. Guo, S. A. DiBenedetto, P. Tewari, M. T. Lanagan, M. A. Ratner, and T. J. Marks, "Nanoparticle, Size, Shape, and Interfacial Effects on Leakage Current Density, Permittivity, and Breakdown Strength of Metal Oxide−Polyolefin Nanocomposites: Experiment and Theory," Chem. Mater., Vol. 22, No. 4, pp. 1567–1578, 2010.

[20] C.-W. Nan, Y. Shen, and J. Ma, "Physical Properties of Composites Near Percolation," Annu. Rev. Mater. Res., Vol. 40, No. 1, pp. 131–151, 2010.

[21] R. Kumar, H. K. Chakerwarti, and N. Gupta, "Improvement of dielectric performance of Silicone rubber by incorporation of nano-sized fillers," IEEE Int'l. Women In Engineering Conf. Electr. Computer Eng. (WIECON-ECE), pp. 147–150, 2015.

[22] J. Lu, "High dielectric constant polymer nanocomposites for embedded capacitor applications," Ph.D. Thesis, Georgia Institute of Technology, USA, 2008.

[23] K. Yu, H. Wang, Y. Zhou., Y. Bai, and Y. Niu, "Enhanced dielectric properties of BaTiO3/poly(vinylidene fluoride) nanocomposites for energy storage applications," J. Appl. Phys., Vol. 113, No. 3, p. 34105, 2013.

[24] C.-C. Li, S.-J. Chang, J.-T. Lee, and W.-S. Liao, "Efficient hydroxylation of BaTiO3 nanoparticles by using hydrogen peroxide," Colloids Surfaces A Physicochem. Eng. Asp., Vol. 361, No. 1, pp. 143–149, 2010.

[25] S.-J. Chang, W.-S. Liao, C.-J. Ciou, J.-T. Lee, and C.-C. Li, "An efficient approach to derive hydroxyl groups on the surface of barium titanate nanoparticles to improve its chemical modification ability.," J. Colloid Interface Sci., Vol. 329, No. 2, pp. 300–5, 2009.

[26] F. Müller, C. A. Ferreira, D. S. Azambuja, C. Alemán, and E. Armelin, "Measuring the proton conductivity of ion-exchange membranes using electrochemical impedance spectroscopy and through-plane cell.," J. Phys. Chem. B, Vol. 118, No. 4, pp. 1102–12, 2014.

[27] "ASTM D120 - 14a. Standard Specification for Rubber Insulating Gloves." ASTM, West Conshohocken, PA, USA, pp. 1–9, 2014.

[28] IEC, "IEC 60903:2014. Live working - Electrical insulating gloves." IEC, p. 117, 2014.

[29] S. Singha and M. Thomas, "Dielectric properties of epoxy nanocomposites," IEEE Trans. Dielectr. Electr. Insul., Vol. 15, No. 1, pp. 12–23, 2008.

[30] C. Xing, J. You, Y. Li, and J. Li, "Nanostructured Poly(vinylidene fluoride)/Ionic Liquid Composites: Formation of Organic Conductive Nanodomains in Polymer Matrix," J. Phys. Chem. C, Vol. 119, No. 36, pp. 21155–21164, 2015.

[31] ASTM, "ASTM D257 – 07 Standard Test Methods for DC Resistance or Conductance of Insulating Materials 1." ASTM, West Conshohocken, Pennsylvania, Pennsylvania, USA, pp. 1–18, 2007.

[32] L. A. Dissado and J. C. Fothergill, *Electrical Degradation and Breakdown in Polymers*, Editor Peter Peregrinus Ltd., United Kingdom, 1992.

[33] E. L. Kowalski, R. Robert, J. Tomioka, J. J. A. Teixeira, J. C. Tosin, R. E. Clerise, and O. E. Filho, "Natural rubber electrical conduction mechanism

in high and low electric fields," Int'l. Sympos. Electr. Insulating Materials, (ISEIM)., Vol. 1, p. 33–35 Vol. 1, 2005.
[34] O. G. Reid, K. Munechika, and D. S. Ginger, "Space charge limited current measurements on conjugated polymer films using conductive atomic force microscopy.," Nano Lett., Vol. 8, No. 6, pp. 1602–9, 2008.
[35] H.-K. Chan, *Ferroelectrics - Characterization and Modeling*, "A General Conductivity Expression for Space-Charge-Limited Conduction in Ferroelectrics and Other Solid Dielectrics", Ch. 4, InTech Publisher, 2011.
[36] D. Q. Tan, Y. Cao, X. Fang, P. C. Irwin, D. Q. Tan, Y. Cao, X. Fang, and P. C. Irwin, "Tunable Nanodielectric Composites," Adv. Mater. Sci. Eng., Vol. 2014, pp. 1–6, 2014.
[37] S. S. Bamji, "Luminescence and Space Charge Phenomena in Polymeric Dielectrics," IEEE Conf. Electr. Insul. Dielectr. Phenomena, pp. 1–12, 2008.
[38] T. Tanaka, "Space charge injected via interfaces and tree initiation in polymers," IEEE Trans. Dielectr. Electr. Insul., Vol. 8, No. 5, pp. 733–743, 2001.
[39] F. Tian, J. Yao, P. Li, Y. Wang, M. Wu, and Q. Lei, "Stepwise electric field induced charging current and its correlation with space charge formation in LDPE/ZnO nanocomposite," IEEE Trans. Dielectr. Electr. Insul., Vol. 22, No. 2, pp. 1232–1239, 2015.
[40] S. Peng, J. He, J. Hu, X. Huang, and P. Jiang, "Influence of functionalized MgO nanoparticles on electrical properties of polyethylene nanocomposites," IEEE Trans. Dielectr. Electr. Insul., Vol. 22, No. 3, pp. 1512–1519, 2015.
[41] G. Chen, D. Tony, L. Shengtao, and L. Zhong, "Space charge in nanodielectrics and its impact on electrical performance," IEEE 11th Int'l. Conf. Properties and Applications of Dielectr. Materials (ICPADM), pp. 36–39, 2015.
[42] L. K. H. Pallon, A. T. Hoang, A. M. Pourrahimi, and E. Al, "The impact of MgO nanoparticle interface in ultra-insulating polyethylene nanocomposites for high voltage DC cables," J. Mater. Chem. A, Vol. 4, No. 22, pp. 8590–8601, 2016.
[43] W. Wang, D. Min, and S. Li, "Understanding the conduction and breakdown properties of polyethylene nanodielectrics: effect of deep traps," IEEE Trans. Dielectr. Electr. Insul., Vol. 23, No. 1, pp. 564–572, 2016.
[44] Prateek [He/She has no initials], V. K. Thakur, and R. K. Gupta, "Recent Progress on Ferroelectric Polymer-Based Nanocomposites for High Energy Density Capacitors: Synthesis, Dielectric Properties, and Future Aspects," Chem. Rev., Vol. 116, No. 7, pp. 4260–4317, 2016.
[45] X. Huang, P. Jiang, and T. Tanaka, "A review of dielectric polymer composites with high thermal conductivity," IEEE Electr. Insul. Mag., Vol. 27, No. 4, pp. 8–16, 2011.
[46] J. Kuffel, W. S. Zaengl, and P. Kuffel, *High Voltage Engineering Fundamentals*, Second Ed. Oxford: Newnes, 2000.
[47] E. Cherney, R. Gorur, A. Krivda, S. Jayaram, S. Rowland, S. Li, M. Marzinotto, R. Ghunem, and I. Ramirez, "DC inclined-plane tracking and erosion test of insulating materials," IEEE Trans. Dielectr. Electr. Insul., Vol. 22, No. 1, pp. 211–217, 2015.
[48] G. Heger, H. Vermeulen, J. Holtzhausen, and W. Vosloo, "A comparative study of insulator materials exposed to high voltage AC and DC surface discharges," IEEE Trans. Dielectr. Electr. Insul., Vol. 17, No. 2, pp. 513–520, 2010.
[49] R. Sarathi, R. K. Sahu, and P. Rajeshkumar, "Understanding the thermal, mechanical and electrical properties of epoxy nanocomposites," Mater. Sci. Eng. A, Vol. 445, pp. 567–578, 2007.
[50] D. Liu, A. M. Pourrahimi, L. K. H. Pallon, C. C. Sánchez, R. T. Olsson, M. S. Hedenqvist, L. Fogelström, E. Malmström, and U. W. Gedde, "Interactions between a phenolic antioxidant, moisture, peroxide and crosslinking by-products with metal oxide nanoparticles in branched polyethylene," Polym. Degrad. Stab., Vol. 125, pp. 21–32, 2016.

N. González Gómez was born in Cumaná - Sucre, Venezuela in 1981. She received the Bachelor in Chemistry from the University of Oriente (2007, Venezuela). During 2008-2010), she was a researcher assistant at the Institute of Basic Research IIBCAUDO, University of Oriente (Venezuela). She obtained the M.S.degree in Applied Chemistry and Polymeric Materials and M.S. of Renewable Materials Engineering from the University of the Basque Country UPV/EHU (Donostia-San Sebastian). Nowadays she is a researcher at Chemical Engineering department of the Universitat Politècnica de Catalunya.

J.-R. Riba (M'09) was born in Igualada, Spain in 1966. He received the M.S. degree and the Ph.D. degree in Physics from the Universitat de Barcelona, Barcelona, Spain, in 1990 and 2000, respectively. In 1992, he joined the Escola d'Enginyeria d'Igualada, Universitat Politècnica de Catalunya (Spain), as an Associate Professor and the Electric Engineering Department in 2001. He belongs to the Motion and Industrial Control Group (MCIA). His research interests include, high voltage engineering, modeling and simulation of electromagnetic devices and electrical machines.

MA. Custal was born in Girona, Spain in 1979. She received the Chemical Engineering degree from the Universitat Politècnica de Catalunya and the DEA degree in Process Engineering from the École Nationale Superieure Industries Chimiques in Nancy (FR) in 2001. She has more than 10 years of experience in the analysis and control of chemical processes with special emphasis on process optimization and chemical process safety. She has developed her experience at R&D, Production & Engineering departments from different EU chemical manufacturing plants. Nowadays she belongs to Sicame group as Responsible of R&D from one of its subsidiary companies in Europe.

Elaine Armelin is Associate Professor in the Chemical Engineering Department and in the Barcelona Research Center in Multiscale Science and Engineering, at the Universitat Politècnica de Catalunya (UPC-Spain). She received her Bachelor's degree in Chemistry in 1995 and Master Degree in Organic Chemistry in 1997, at the Universidade de São Paulo (USP-Brazil). In 1997 she moved to Barcelona to perform her PhD studies in Polymer Science at UPC. Her current work focuses on the developing of hybrid materials with mainly applications within the life sciences and for energy storage, as well as in the development of new organic-inorganic coatings to protect metals and alloys against corrosion.